



## Design, molecular docking, synthesis, and *in vitro* pharmacological evaluation of biomolecules-histone deacetylase inhibitors conjugates with carbohydrazide as a novel zinc-binding group

Ameer H. Alwash<sup>a\*</sup>, Noor Hatf Naser<sup>b</sup>, Munaf H. Zalzal<sup>c</sup>

<sup>a</sup>Department of pharmaceutical chemistry, College of Pharmacy, Albayan University, Baghdad, Iraq

<sup>b</sup>Department of pharmaceutical chemistry, Faculty of Pharmacy, University of Kufa, Najaf, Iraq

<sup>c</sup>Department of pharmacology and toxicology, College of Pharmacy, University of Baghdad, Iraq

### Abstract

Histone deacetylase inhibitors (HDACIs) are newly emerging chemotherapeutic agents which have shown great potential in the treatment of many types of cancers. However, these agents have many drawbacks which may limit their clinical application such as low oral bioavailability, and low intracellular concentration in solid tumors which may require high doses leading to side and maybe toxic effects. Additionally, their zinc-binding group (ZBG) is partly responsible partly for their poor physicochemical properties. *In silico* design, synthesis, and characterization of new HDACIs involving biomolecules (biotin and phenylalanine) with carbohydrazide as a novel ZBG were achieved successfully and hopefully, to increase the targetability and to overcome the limitations of traditional hydroxamate-based HDACIs. MTT assay of compounds **2c** and **3d** (which are biotin and phenylalanine-linked derivatives respectively) showed higher antiproliferative activity than SAHA and 5-FU against MCF7 and lower cytotoxic effect against NHF cell lines which were consistent with the docking study results. Additionally, compound **1b** displayed comparable cytotoxic results to SAHA against MCF7 and NHF. These results were found to be encouraging for the involvement of biomolecules in the future development of HDACIs. Therefore, carbohydrazide as a ZBG could be thought of as a counterpart to hydroxamate moiety and may be considered as a successful replacement for hydroxamate moiety upon designing new HDACIs.

Keywords: Histone deacetylase inhibitors; Zinc-binding group; cancer-targeting; phenylalanine; biotin

### 1. Introduction

Histone deacetylases (HDACs) are a family of epigenetic Zn-dependent enzymes that are composed of eighteen different isoforms which have an important role in epigenetic modifications [1]. To date, 18 isoforms of HDACs (1-18) were identified and classified according to their homology, structure diversity, and sequence, into four classes (I-IV): class I (1,2,3, and 8), II (IIa: 4,5,7, and 9, IIb: 6 and 10), and IV (11) are Zn-dependent HDACs, also termed as reduced potassium dependency-3/Histone deacetylase-a1 family (Rpd3/Hda1 family) while class III is composed of nicotinamide adenine dinucleotide (NAD<sup>+</sup>)-dependent sirunits (SIRT 1-7)[2]. It has been found that inhibiting the activity of HDAC enzymes affects the equilibrium between the opposing actions of histone acetylases (HATs) and HDACs which lead to the shifting toward the predominancy of HATs

activity, and consequent induction of histone and non-histone proteins acetylation. Therefore, gene expression will be affected through the stimulation and/or silencing of some genes which change the expression of transcription factors and specific proliferative and/or apoptotic genes[3]. This will induce apoptotic pathways, bring cancer cells into cell cycle arrest, differentiation, reduce angiogenesis, stimulate DNA fragmentation, and inhibition of DNA repair leading to cell death.[4], [5]. Consequently, histone deacetylase inhibitors (HDACIs) have emerged as a new group of chemotherapeutic agents which have revealed a potent anticancer activity and some of them acquired FDA approval for treatment of different types of cancers. The first one was vorinostat (also known as suberoylanilide hydroxamic acid or shortly abbreviated as SAHA) [6]. Nevertheless, HDACIs have shown drawbacks that limit their

\*Corresponding author e-mail: [ameer.hussein@albayan.edu.iq](mailto:ameer.hussein@albayan.edu.iq)

Receive Date: 05 November 2021, Revise Date: 11 February 2022, Accept Date: 25 February 2022

DOI: 10.21608/EJCHEM.2022.104511.4830

©2022 National Information and Documentation Center (NIDOC)

clinical prevalence for the treatment of cancer such as, poor pharmacokinetic properties, for example, vorinostat is extensively metabolized by the liver and it has low aqueous solubility (0.2 mg/ml in 25 °C and pH 7) and permeability ( $\log p = 1.9$ ) which leads to low oral bioavailability (11% for rats and 43% for humans), low intracellular concentrations (especially in solid tumors) which require higher doses to achieve effective levels resulting in adverse effects (such as, fatigue, thrombocytopenia, diarrhea, nausea, and cardiotoxicity) and make injectable dosage forms difficult to prepare[7].

HDACIs share common general structural features which are composed of three main pharmacophoric moieties mimicking the natural peptide substrates: a protein surface recognition moiety, also termed as "cap" unit, a Zinc-binding group (ZBG), and a hydrophobic linker [8].

ZBG coordinates with the catalytic  $Zn^{2+}$  which is situated at the end of the pocket of the active site leading to hinder the enzyme catalytic activity [9]. Various ZBGs have been reported and investigated, however, there are classical moieties such as hydroxamic acid[10], benzamide[11], thiol[12], carboxylic acid[13] and trifluoromethyl ketone[14]. ZBG could affect the potency, selectivity, and pharmacokinetic properties of the HDACI agent, for example, benzamide inhibitors have higher HDAC3 selectivity than the FDA-approved hydroxamic acid derivatives but generally have less receptor affinity and potency[15]. Hydroxamic acids and benzamides are the most known, widely distributed, and investigated as anticancer agents[16, 17].

Biomolecules (also known as biological molecules) is a term that covers a wide range of compounds produced by living cells (such as, vitamins, amino acids, nucleic acids, fatty acids, saccharides, and their polymers) to perform a wide array of cellular functions[18]. They could have a vital role in maintaining all aspects of the cellular environment and homeostasis such as energy storage, cellular growth and support, signal transduction, catalysis of cellular biochemical reactions, DNA transcription and repair, and many others[19]. Due to the high metabolic and proliferative rate of cancer cells, their need for biomolecules is crucial. Therefore, they have highly overexpressed receptors and cellular internalization mechanisms[20]. For this reason, biomolecules have been utilized as drug delivery molecules and involved in designing various anticancer compounds to overcome the drawbacks of traditional chemotherapeutic agents most importantly low targetability with consequent side effects and high toxicity[21]. Furthermore, specific biomolecules may have attractive properties which encourage drug designers to use them in developing biomolecules-

anticancer drug conjugates.

Carbohydrazide (CHZ) is an interesting azotic chain ligand with several lone-pair electrons. CHZ is hydrazine, which has more functional groups. CHZ may coordinate with many metal ions in a monodentate or multidentate pattern (figure 1)[22].

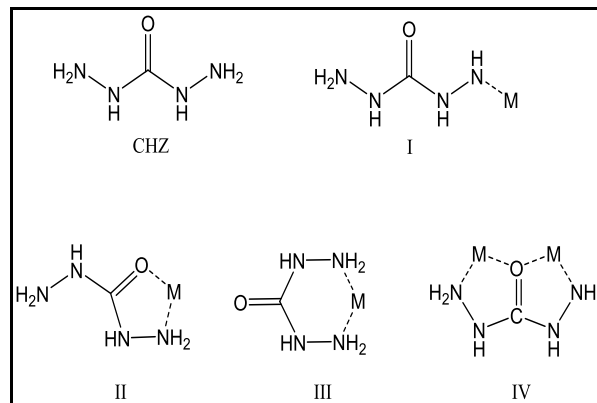


**Figure 1.** Chemical structure and coordination models of CHZ. Dashed lines and M represent coordinative bonds and a heavy metal ion respectively. I, (II and III), and IV represent mono, bi, and multidentate interaction of CHZ with M.

In this work, water-soluble vitamin biotin and amino acid, phenylalanine (Phe), have been chosen due to their favorable characteristics such as ease of manipulation, and high safety profile[23]. It has been proposed that the conjugation with these biomolecules will make them act as a carrier for the designed HDACIs which leads to an increase in their uptake by cancer cells (leading to an increase in the targetability and intracellular concentration of the designed compounds in cancer cells), and the new compounds may have an improved physicochemical property.

Additionally, CHZ was involved in the design of new HDACIs as a novel ZBG, hopefully, to overcome the limitations of hydroxamate moiety (such as *in vivo* instability) and improve the anticancer activity of the designed compounds.

## 2. Experimental

Reagents and solvents used in chemical synthesis obtained from suppliers: Central drug house (P) Ltd. (India), Otto Chemie Pvt Ltd. (India), BHD laboratory reagent (England), Beijing Yibai Biotechnology (China), Sigma Aldrich (Germany), Chem-Lab (Belgium), and Thomas Barker (UK). Melting points were measured (uncorrected) by using an electrical melting point apparatus (Electrothermal 9300, USA).

Thin-layer chromatography was achieved using 0.2 mm pre-coated TLC plates (Merck, Germany). FT-IR spectroscopy was carried out by using an FT-IR affinity-1 spectrophotometer (Shimadzu, Japan) and was kindly performed by the college of pharmacy / University of Baghdad.  $^1\text{H}$  and  $^{13}\text{C}$ -NMR spectra were recorded using NMR Bruker 500 MHz-Avance III ( $d_6$ -DMSO as a solvent) and chemical shifts were recorded in parts per million (ppm).  $^1\text{H}$  and  $^{13}\text{C}$ -NMR analyses were kindly performed by the faculty of science / University of Jordan. Tetramethyl silane was used as a reference.

Molecular docking was performed using the GOLD software program (Hermes 2020.3.0.) and the 3D structure of the target enzymes (HDACs 2 and 10) was obtained and retrieved from the protein data bank (PDB) website (PDB ID: 4LXZ and 6WBQ respectively)[24].

Cytotoxicity assay was performed using fetal bovine serum (Capricorn, Germany), RPMI 1640, trypsin/EDTA; 3-(4,5-dimethyl-2-thiazolyl)-2,5-diphenyl -2H-tetrazolium bromide (MTT stain-Bio-World, Dublin, OH, USA); cell culture plates (Santa Cruz Biotechnology), dimethyl sulfoxide (DMSO-Santacruz Biotechnology, Dallas, TX, USA), microtiter reader (Gennex lab., Srinagar Colony Hyderabad, India), CO<sub>2</sub> incubator and laminar flow hood (Cypress Diagnostics, Hulshout, Belgium). It was kindly carried out at the iRAQ Biotech laboratories, Baghdad, Iraq.

## 2.1. Molecular docking

Drawing of the 2D chemical structure of the designed compounds and their energy minimization were carried out by Chem3D (version: 19.1.1.21) and they were saved in SYBYL2 (mol2) format. The 3D structure of the target enzymes (HDACs 2 and 10) was obtained and retrieved from the protein data bank (PDB) website (PDB ID: 4LXZ and 6WBQ respectively) and uploaded to the GOLD software program (Hermes 2020.3.0.). Hydrogen atoms were added and unnecessary metals (except  $\text{Zn}^{2+}$ ), ligands (except SAHA and Tubastatin A (TubA)), enzyme chains (except chain A), and water molecules were deleted (except HOH 561, 606, and 791 for HDAC2 and HOH 849 and 947 for HDAC10 which were extracted for docking). The binding site was defined by the reference ligand for each enzyme (SAHA and TubA for HDACs 2 and 10 respectively) and cavity size was determined by all atoms within 6 Å. The saved compounds (mol2 format) were uploaded and the GOLD run was allowed to proceed. When the run was completed, the highest PLP scores for each compound and their images (which show the

interaction of each compound with the  $\text{Zn}^{2+}$  and amino acid residues in the binding site) were recorded.

## 2.2. Chemical synthesis (scheme 1 and 2)

### 2.2.1. Chemical synthesis of methyl 4-(aminomethyl)benzoate hydrochloride (MAB)

This compound was synthesized by an esterification reaction of amino acids using thionyl chloride to produce the required product as HCl salt as follows[25]:

4-(aminomethyl) benzoic acid (4.53g, 30 mmol) was suspended in 70 ml of anhydrous methanol and cooled to 5 °C. Thionyl chloride (2.6 ml, 36 mmol) was added dropwise over 15 min. The reaction mixture was allowed to stir at room temperature for 30 min then refluxed for 3 h. The solvent was then evaporated under reduced pressure and the produced residue was washed (30 ml\*3) by methanol: ethyl acetate (1:3) dried and collected.

### 2.2.2. Chemical synthesis of compounds 2a and 3a

These compounds were synthesized by the mixed anhydride method for amide formation by using methyl chloroformate (MCF) as follows[26]:

Triethylamine (TEA) (1.4 ml, 10 mmol) was added to a solution of *para*-aminobenzoic acid (PABA) (1.37 g, 10 mmol) in anhydrous tetrahydrofuran (THF) (20 ml) at 25 °C. The mixture was stirred for 15 min and cooled to -5 °C. To a stirred solution of (biotin for compound **2a** and N-[(Tert-Butoxy)carbonyl]-L-phenylalanine (boc-phe) for compound **3a**) (10 mmol) in anhydrous dimethylformamide (DMF) (30 ml) and TEA (1.4 ml, 10 mmol) in an ice bath at -5 °C, MCF (0.77 ml, 10 mmol) was added dropwise over 15 min and the reaction was further stirred for 15 min. Afterward, the previously dissolved and cooled PABA portion was added dropwise over 30 min then the reaction mixture was removed from the ice bath and left to stir overnight at room temperature. The following day, some of the solvent mixture was evaporated under reduced pressure and cold distilled water (DW) was added to induce precipitation. The precipitate was washed with 5% HCl, recrystallized by DW, dried, and collected.

### 2.2.3. Chemical synthesis of compounds 1a, 2b and 3b

TEA (1.4 ml, 10 mmol) was added to a suspension of MAB (1 g, 5 mmol) in anhydrous chloroform (15 ml) at 25 °C. The mixture was stirred for 15 min and cooled to -5 °C. To a stirred solution of the compound containing the carboxylic acid ((benzoic acid for compound **1a**), (**2a** for compound **2b**), and (**3a** for compound **3b**)) (5 mmol) in anhydrous chloroform (20 ml) and TEA (0.7 ml, 5 mmol) in an ice bath at -5 °C, MCF (0.39 ml, 5 mmol) was added dropwise and the

reaction was further stirred for 30 min. Afterward, the previously dissolved and cooled MAB portion was added dropwise over 30 min then the reaction mixture was removed from the ice bath and left to stir overnight at room temperature. The solvent was evaporated under reduced pressure and the produced residue was washed with 5% NaHCO<sub>3</sub> followed by 5% HCl and DW. After filtration, the product was dried (by oven) and collected.

#### 2.2.4. Chemical synthesis of compounds **1b**, **2c** and **3c**

These compounds were synthesized by the reaction of a hydrazine-containing compound with an ester [27]. KOH (0.19 g, 3.5 mmol) was dissolved in 4 ml DW and added gradually to a suspension of compound (**1a** for **1b**, **2b** for compound **2c** or **3b** for compound **3c**) (1 mmol) and CHZ (2.7 g, 30 mmol) in 16 ml of methanol with continuous stirring. The mixture was refluxed for 6 hrs and till the completion of the reaction, which was monitored by TLC. The solvent was evaporated and the produced residue was washed with ethyl acetate, dried, recrystallized by DW, and collected.

#### 2.2.5. Chemical synthesis of compound **3d**

The synthesis of this compound was carried out by deblocking reaction of the Boc group to produce a free amine group which is as follows [28]:

Compound **3c** (0.29 g, 0.5 mmol) was dissolved in 2 ml chloroform containing anisole (2 drops, 0.5 mmol) and cooled to 0 °C then 8 ml of TFA was added gradually with continuous stirring over 30 min and the reaction mixture was further stirred for another 30 min at room temperature. The reaction was monitored by TLC which confirmed the success of Boc deblocking by the disappearance of compound **3c** spot. Cold DW was added to the reaction mixture and neutralized by 5% NaHCO<sub>3</sub> to induce precipitation of the product which was filtered, recrystallized by ethanol, and collected.

### 2.3. In vitro cytotoxicity study

#### 2.3.1. Maintenance of cell cultures

MEM was used in maintaining Michigan cancer Foundation-7 (MCF-7) cell line and supplemented with 100 µg/mL streptomycin, 100 units/ml penicillin, and 10% Fetal bovine. The passage of cells was carried out by using reseeded Trypsin-EDTA at 50% confluence twice a week and incubated at 37 °C [29].

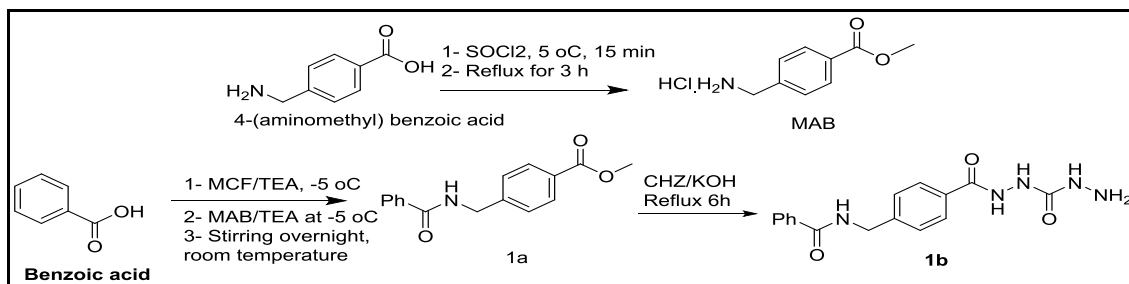
#### 2.3.2. Combination Cytotoxicity Assays

For the determination of the cytotoxic effect of the synthesized compounds, a 96-well plates conducted-MTT cell viability study was performed [30]. Cells were seeded at  $1 \times 10^4$  cells/well and treated with the tested compounds (**1b**, **2c**, **3d**, SAHA, and 5-fluorouracil (5-FU)) after 24 h or the confluence of a monolayer. After 72 h of treatment, the medium was removed and 28 µL of 2 mg/mL solution of MTT was added to measure cells viability. They were incubated for 1.5 h at 37 °C. MTT solution was removed and 130 µL of dimethyl sulfoxide (DMSO) was added to solubilize the remaining crystals in the wells followed by incubation and shaking for 15 min at 37 °C [31]. To measure the absorbency, a microplate reader at 492 nm (test wavelength); the cytotoxicity assay was carried out in triplicate. To determine the rate at which the cell growth was inhibited, the percentage of cytotoxicity was calculated by using the following equation: equation [31], [32] -

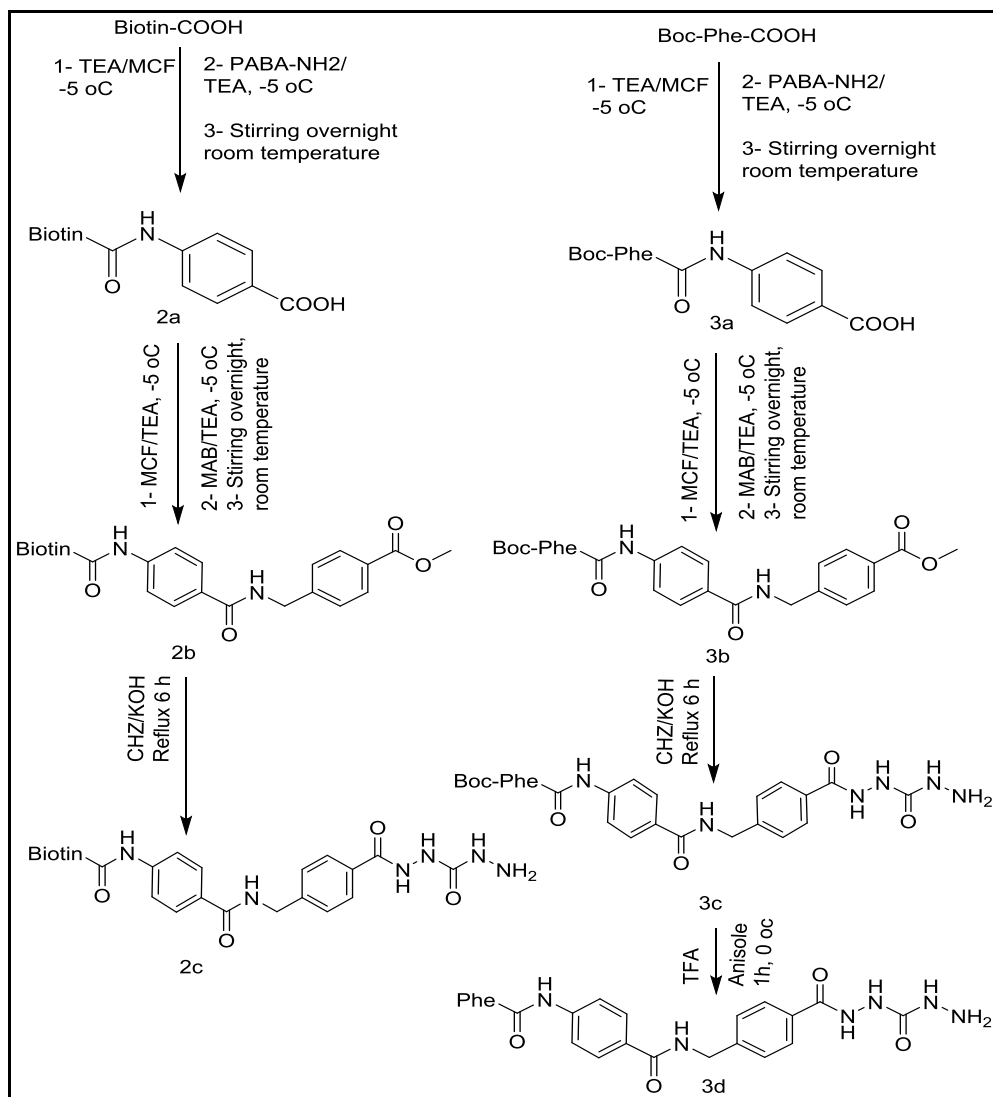
$$\% \text{Cell viability} = (\text{Absorbance of treated cell} / \text{Absorbance of non-treated cell}) \times 100$$

$$\% \text{Cytotoxicity} = 100 - \text{cell viability}$$

The shape of cells was visualized under an inverted microscope, 96-well microtitration plates were seeded by 200 µL of cell suspensions at density  $1 \times 10^4$  cells/mL and incubated for 48 h at 37 °C. Afterward, the medium was removed and each of the tested compounds was added at its (IC<sub>50</sub>) separately. After the exposure time, the plates were stained with 50 µL of crystal violet solution and incubated at 37 °C for 15 min. Then, the dye was removed by gentle washing with water. Finally, the cells were examined by an inverted microscope with 40× field magnification, and images were recorded by using a digital camera [33].



**Scheme 1.** Chemical synthesis of MAB and series 1 compounds (**1a** and **1b**).



**Scheme 2.** Chemical synthesis of series 2 and 3 compounds.

### 2.3.3. Statistical analysis:

The obtained data were statically analyzed using an unpaired t-test with GraphPad Prism 9. The values were presented as the mean  $\pm$  SD of triplicate measurements.

## 3. Results and discussion

### 3.1. Molecular docking

A molecular docking study has been performed to explore the binding fitness of the designed compounds with the selected targets (HDACs). Currently, researchers are focusing on developing selective HDACs inhibitors to overcome the limitations of traditional pan-inhibitors such as undesirable side effects and toxicity as well as improving their physicochemical properties. In our work, these limitations were highlighted to suggest a new

approach to overcome those drawbacks by using biomolecules.

Therefore, the HDAC isoform selectivity approach was not fundamental in our point of view. On the other hand, the level of overexpression of each HDAC isoform was a critical issue. It has been found that HDAC 2 and 10 have a very high incidence of overexpression (maybe the highest) in cancer patients among class I and II members respectively[34]. Consequently, they were chosen as docking targets.

The molecular docking study has been carried out by using GOLD software program (Hermes 2020.3.0.) and PLP fitness as a scoring function. PLP is a dimensionless scoring function in which a higher score means a better docking result and a fitter pose[35], [36]. Docking scores (PLP fitness scores) and docking data are listed in table 1.

SAHA was included as a reference ligand for analysing the docking scores of the designed compounds with the two targets (HDACs 2 and 10).

Regarding HDAC2, SAHA exhibited a docking score (83.24). All the compounds have displayed higher docking scores than SAHA and compound **1b** has shown the highest score among all the docked ligands (92.91).

Regarding HDAC 10, SAHA exhibited a docking score (85.84). All the designed compounds have shown docking scores higher than that of SAHA and compound **3d** has shown the highest score among all the docked ligands (114.52).

The visualization images (figures 2 to 5) have displayed that the conformation of all designed

compounds in the catalytic pocket and their binding to the catalytic metal (zinc ion) and the surrounding amino acid residues are similar to that of SAHA (as shown by the red and blue colored amino acid residues in table 1). Therefore, the high docking scores, as well as, the ligand-receptor binding patterns of the designed compounds (which was comparable to that of SAHA-receptor binding), have provided strong evidence about the potential anticancer activity of the designed compounds and were found to be encouraging to move forward with the chemical synthesis of the designed compounds and performing *in vitro* pharmacological activity.

**Table 1.** Docking scores and bonds length of compounds-amino acids residues interaction in the active site of HDACs 2 and 10.

Comp.	PLP fitness	H-bonds and their distance (Å°)	Short contacts and their distance (Å°)
HDAC2			
SAHA	83.24	Asp104* (2.752), His145 (2.50), His146 (2.613), Asp181 (2.98 and 2.729), His183 (3.04), Asp269 (2.899), Tyr308 (2.566)	Zn401 (1.957 and 2.331)
<b>1b</b>	92.91	Asp104 (3.008), His145 (2.487 and 3.071), Gly154 (2.621 and 2.956), Asp181 (2.32), His183 (3.04 and 3.05), Asp269 (3.032), Tyr308 (2.804)	Zn401 (2.2)
<b>2c</b>	84.42	His146 (2.98 and 3.009), Gly154 (2.795), His183 (2.694), Glu208 (2.923), Tyr308 (2.761)	Zn401 2.193
<b>3d</b>	84.48	His145 (2.946 and 3.087), Gly154 (2.397 and 2.487), His183 (3.012), Gly306, (2.807), Tyr308 (2.948)	Zn401 (2.334) Asp181 (2.261)
HDAC10			
SAHA	85.84	His136* (3.054), His137 (2.533), Asp174 (2.952), His176 (3.059), Tyr307 (2.703)	Zn712 (2.322)
<b>1b</b>	90.45	His136 (2.557), Gly145 (2.852), Asp174 (2.617), Tyr307 (2.845)	Zn712 (2.394)
<b>2c</b>	93.89	Glu24 (2.686), His136 (2.946 and 2.803), Gly145 (3.046 and 2.793), Asp174 (2.261), Pro206 (2.421), Gly305 (3.033), Tyr307 (2.962)	Zn712 (2.185)
<b>3d</b>	114.52	Ala94 (2.725), His136 (2.791), Gly145 (2.93), Asp174 (2.475), His176 (2.639) Tyr307 (2.693)	Zn712 (2.049)

\* Red and blue colored amino acids residues represent the residues involved in the interaction between SAHA and the active site of HDAC 2 and 10 respectively.

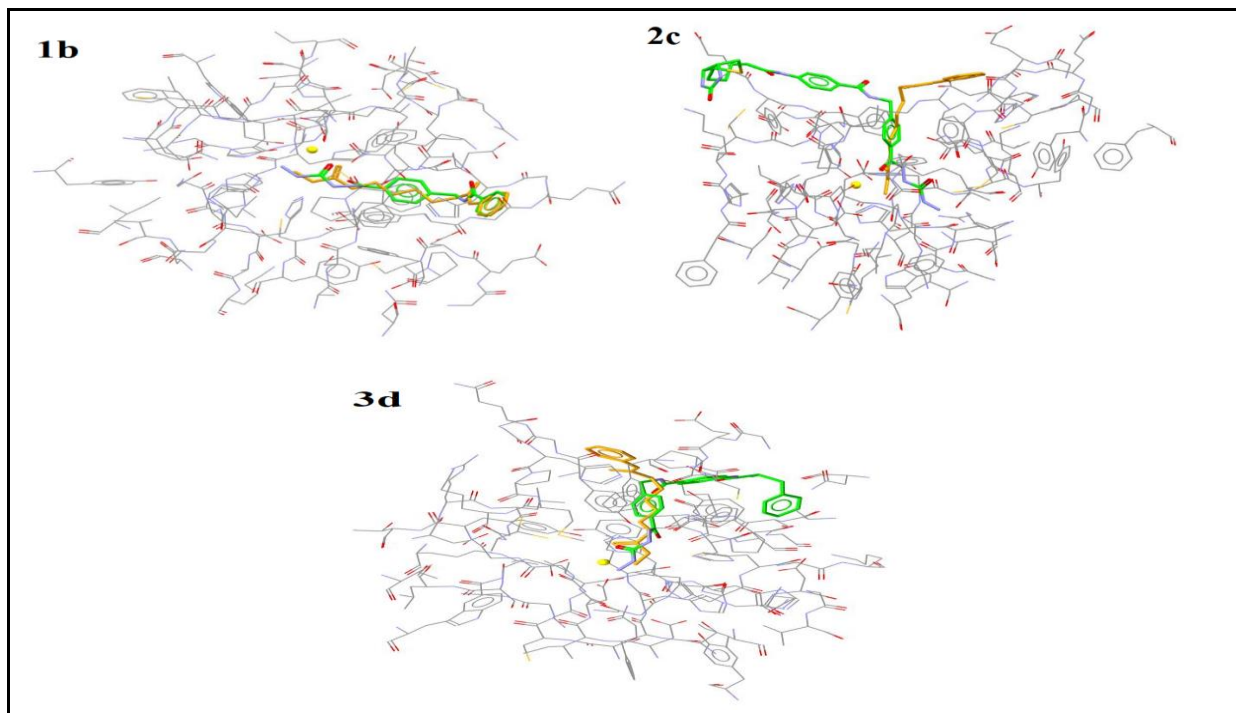


**Figure 2.** Overlay of the designed compounds over SAHA in the catalytic pocket of HDAC2 (PDB ID:4LXZ). Orange and green ligands represent SAHA and the designed compounds respectively. The yellow small ball represents zinc ion.

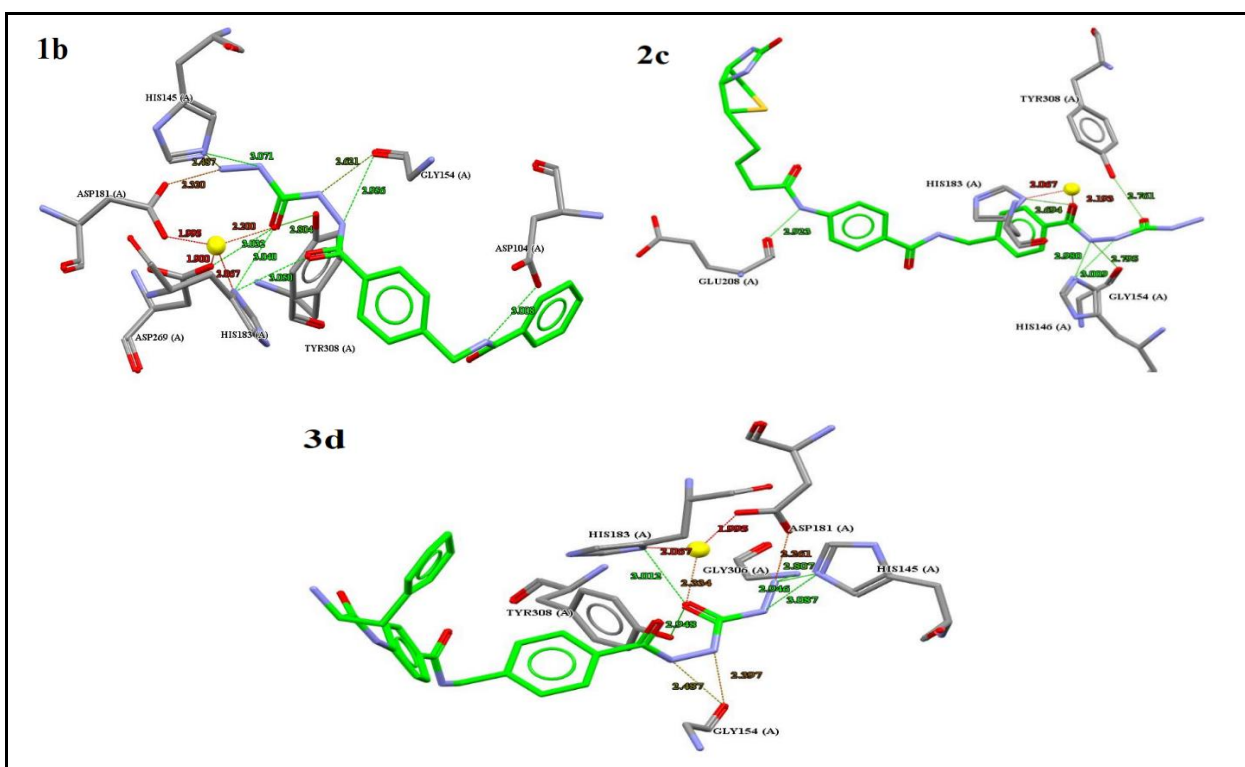


**Figure 3.** Interaction of the designed compounds and SAHA with the amino acids residues of HDAC2 catalytic pocket (PDB ID:4LXZ). Yellow ball, green, and red dashes represent Zn401, H-bonds, and short contacts respectively.

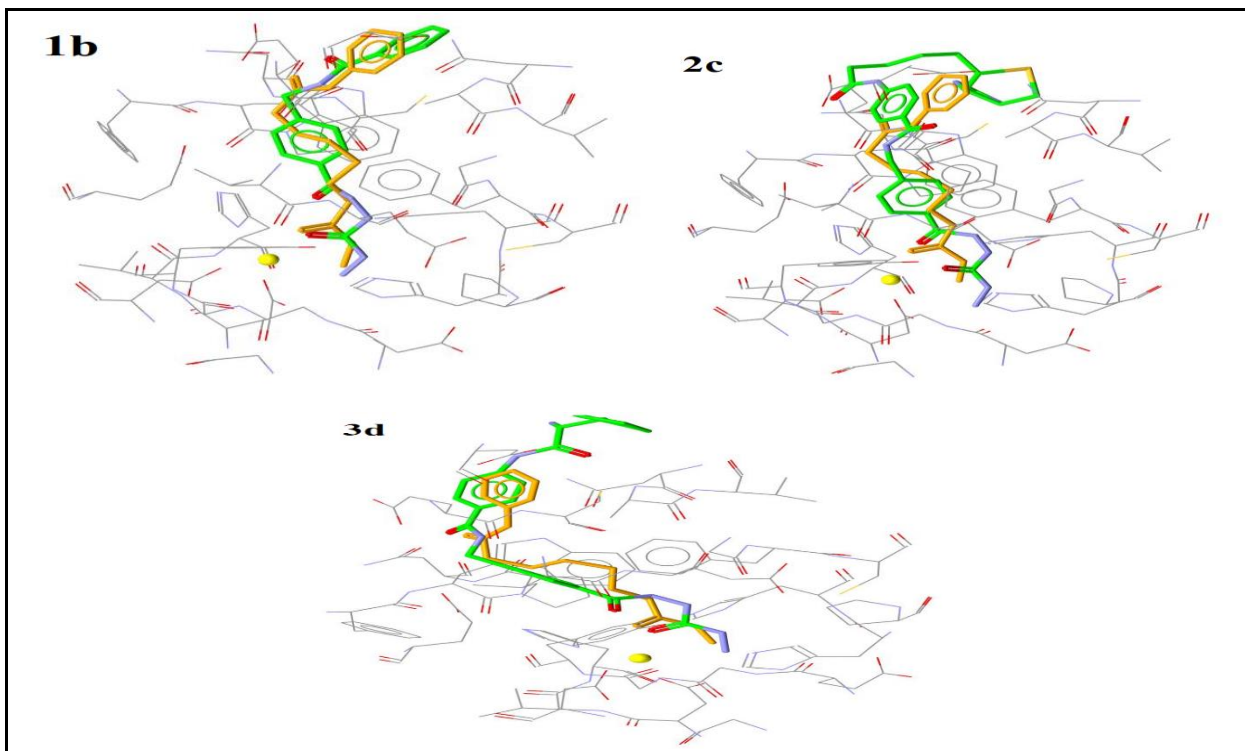


**Figure 4.** Overlay of the designed compounds over SAHA in the catalytic pocket of HDAC10 (PDB ID:6WBQ). Orange and green ligands represent SAHA and the designed compounds respectively. The yellow small ball represents zinc ion.

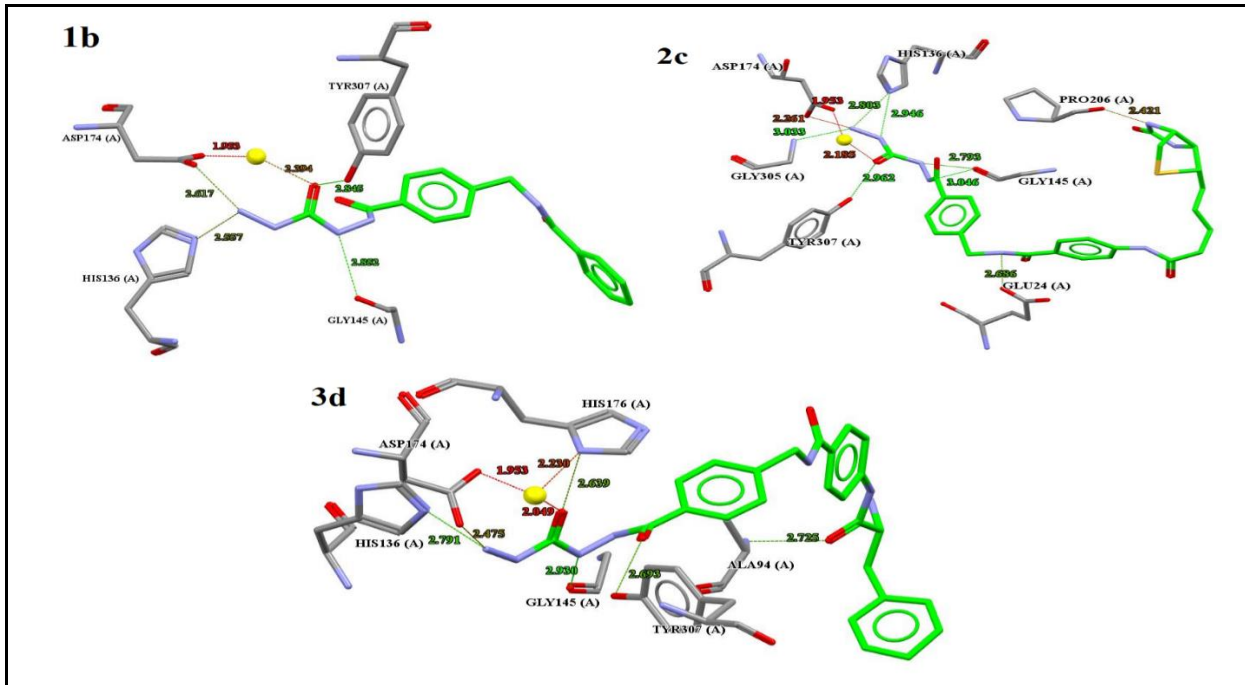


**Figure 5.** Interaction of the designed compounds and SAHA with the amino acid's residues of HDAC10 catalytic pocket (PDB ID:6WBQ). Yellow ball, green, and red dashes represent Zn712, H-bonds, and short contacts respectively.

### 3.2 Chemical synthesis

#### Chemical synthesis of methyl 4-(aminomethyl)benzoate hydrochloride MAB

White crystals, yield 94%, m.p. 250-252 °C. FT-IR (ATR;  $\nu$ ,  $\text{cm}^{-1}$ ): 3005 (aromatic  $\text{sp}^2$  C-H str. vibration), 2958, 2877 (asym. and sym.  $\text{sp}^3$  str. vibration of  $\text{CH}_3$  &  $\text{CH}_2$  groups), 1720 (C=O str. vibration of ester), 1597, 1508 (aromatic C=C str.), 1280 (C-O-C str. vibration of ester).

#### Methyl 4-(benzamido methyl) benzoate 1a

White powder, yield 79%, m.p. 131-133 °C,  $R_f$  0.53 (chloroform: ethyl acetate: methanol; 3:3:4). FT-IR (ATR;  $\nu$ ,  $\text{cm}^{-1}$ ): 3290 (NH str. vibration of benzamide amide), 3066 (aromatic  $\text{sp}^2$  C-H str. vibration), 2951, 2920 (asym. and sym.  $\text{sp}^3$  str. vibration of  $\text{CH}_3$  &  $\text{CH}_2$  groups), 1708 (C=O str. vibration of ester), 1635 (C=O str. vibration of benzamide), 1612, 1543 (aromatic C=C str.), 1280 (C-O-C str. vibration of ester).

#### N-(4-(2-(hydrazine carbonyl) hydrazine-1-carbonyl) benzyl) benzamide 1b

Pale green powder, yield 81%, m.p. 180-182 °C,  $R_f$  0.89 (chloroform: ethyl acetate: methanol; 3:3:4). FT-IR (ATR;  $\nu$ ,  $\text{cm}^{-1}$ ): 3400-3200 (broad NH str. vibration bands of benzamide and CHZ amides and doublet bands of the primary amine), 3089 (aromatic  $\text{sp}^2$  C-H str. vibration), 2945, 2889 (asym. and sym.  $\text{sp}^3$  str. vibration of  $\text{CH}_2$  group), 1685, 1631 (broad C=O str. vibration of benzamide and CHZ respectively), 1527 (broad aromatic C=C str. possibly due to overlap with N-H bending of four amide moieties).  $\text{C}_{16}\text{H}_{17}\text{N}_5\text{O}_3$ ,  $^1\text{H}$ NMR ( $\delta$ , ppm): 12.82 (s, NH, 1H), 11.14 (s, NH, 1H), 9.05 (s, NH, 1H), 8.96 (s, NH, 1H), 7.8-7.3 (m, aromatic CH and  $\text{CH}_2$ , 9H), 4.51 (s,  $\text{NH}_2$ , 2H), 4.48 (s,  $\text{CH}_2$ , 2H).  $^{13}\text{C}$ NMR: 167.6 (C=ONH), 166.7 (C=ONH), 164.6 (CHZ C=O), 134.6-127.4 (aromatic), 42.88 ( $\text{CH}_2$ ).

#### 4-(5-((3aS,4S,6aR)-2-oxohexahydro-1H-thieno[3,4-d]imidazol-4-yl) pentan amido) benzoic acid 2a

Off-white powder, yield 80%, m.p. 239-241 °C. FT-IR (ATR;  $\nu$ ,  $\text{cm}^{-1}$ ): 3400-3200 (broad OH str. vibration of the carboxyl group), 3290, 3255 (NH str. vibration of anilide and urea amides), 3047 (aromatic  $\text{sp}^2$  C-H str. vibration), 2931, 2866 (asym. and sym.  $\text{sp}^3$  str. vibration of  $\text{CH}_2$  group), 1693 (C=O str. vibration of the urea amide), 1666 (broad C=O str. vibration due overlap of carbonyl absorption of the carboxyl and anilide amides), 1597, 1523 (aromatic C=C str.).

#### methyl 4-((4-(5-((3aS,4S,6aR)-2-oxohexahydro-1H-thieno[3,4-d]imidazol-4-yl) pentanamido)benzamido) methyl)benzoate 2b

White powder, yield 75%, m.p. 207-209 °C. FT-IR (ATR;  $\nu$ ,  $\text{cm}^{-1}$ ): 3290 (broad NH str. vibration due to overlap of anilide, urea, and benzamide amides), 1724 (C=O str. vibration of ester), 1697 (C=O str. vibration of the urea amide), 1658 (C=O str. vibration of anilide amide), 1627 (C=O str. vibration of benzamide

amide), 1608, 1523 (aromatic C=C str.), 1280 (C-O-C str. vibration of ester).

#### N-(4-(2-(hydrazinecarbonyl) hydrazine-1-carbonyl) benzyl)-4-(5-((3aS,4S,6aR)-2-oxohexahydro -1H-thieno[3,4-d] imidazol-4-yl) pentanamido) benzamide 2c

White powder, yield 83%, m.p. 250-252 °C. FT-IR (ATR;  $\nu$ ,  $\text{cm}^{-1}$ ): 3400-3200 (broadband due to overlapping of N-H str. vibration of anilide, urea, benzamide amides, and doublet of the primary amine), 2931, 2866 (asym. and sym.  $\text{sp}^3$  str. vibration of  $\text{CH}_2$  group), 1700-1630 (broadband due to the overlap of C=O str. vibration of urea, CHZ, anilide, and benzamide amides), 1597, 1523 (aromatic C=C str.).  $\text{C}_{26}\text{H}_{32}\text{N}_8\text{O}_5\text{S}$ ,  $^1\text{H}$ NMR ( $\delta$ , ppm): 11.59 (s, NH of  $\text{NHC}=\text{O}$  of CHZ, 1H), 10.45 (s, NH of  $\text{Ar}-\text{C}=\text{ONH}$ , 1H), 10.37 (s, NH of  $\text{C}=\text{ONH}-\text{Ar}$ , 1H), 9.09 (s, NH of  $\text{Ar}-\text{C}=\text{ONHCH}_2$ , 1H), 8.48 (s, NH of  $\text{C}=\text{ONHNH}_2$  of CHZ, 1H), 7.8-6.7 (m, aromatic  $\text{CH}_2$ , 8H), 4.47 (q, CH, 1H), 4.26 (t, CH, 1H), 4.19 (s, NH, 2H), 4.09 (s,  $\text{CH}_2$ , 2H), 3.06 (t, CH, 1H), 2.8 (d,  $\text{CH}_2$ , 2H), 2.32 (t,  $\text{CH}_2$ , 2H), 1.6-1.1 (q,  $3\text{CH}_2$ , 6H).  $^{13}\text{C}$ NMR: 172.2 (C=ONH), 167.7 (C=ONH), 166.3 (C=ONH), 163.3 (Biotin  $\text{NHC}=\text{ONH}$ ), 161.2 (CHZ C=O), 139.7-118.6 (aromatic), 61.5 (CH-NH), 59.7 (CH-NH), 58.9 (CH-S), 42.8 ( $\text{CH}_2$ -NH), 40.3 ( $\text{CH}_2$ -S), (36.7, 34.4, 28.5, 25.4) (Biotin  $\text{CH}_2$ ).

#### 4-(2-((tert-butoxy carbonyl) amino)-3-phenylpropanamido) benzoic acid 3a

White powder, yield 71%, m.p. 186-188 °C,  $R_f$  0.67 (hexane: ethyl acetate: methanol; 6: 3: 1). FT-IR (ATR;  $\nu$ ,  $\text{cm}^{-1}$ ): 3400-3200 (broad OH str. vibration of the carboxyl group), 3332, 3248 (NH str. vibration of anilide amide and carbamate), 2981, 2823 (asym.  $\text{sp}^3$  str. vibration of  $\text{CH}_3$  &  $\text{CH}_2$  groups), 1670 (C=O str. vibration of the anilide, carbamate, and carboxyl groups), 1597 and 1519 (aromatic C=C str.).

#### methyl 4-((4-(2-((tert-butoxycarbonyl) amino)-3-phenylpropanamido) benzamido) methyl) benzoate 3b

Pale brown powder, yield 74%, m.p. 163-165 °C,  $R_f$  0.74 (hexane: ethyl acetate: methanol; 6: 3: 1) and 0.28 (chloroform: methanol; 4: 6). FT-IR (ATR;  $\nu$ ,  $\text{cm}^{-1}$ ): 3317 (broad NH str. vibration due to overlap of anilide and benzamide amides and carbamate bands), 1716 (C=O str. vibration of ester), 1685 (C=O str. vibration of the anilide amide), 1666 (C=O str. vibration of carbamate), 1631 (C=O str. vibration of benzamide amide), 1600, 1523 (aromatic C=C str.), 1276 (C-O-C str. vibration of ester).

#### tert-butyl (1-((4-(2-(hydrazinecarbonyl) hydrazine-1-carbonyl) benzyl) carbamoyl) phenyl) amino)-1-oxo-3-phenylpropan-2-yl) carbamate 3c

Pale green powder, yield 79%, m.p. 195-197 °C,  $R_f$  0.69 (chloroform: methanol; 4: 6). FT-IR (ATR;  $\nu$ ,  $\text{cm}^{-1}$ ): 3400-3100 (broadband due to overlapping of N-H str. vibration bands of anilide, CHZ, benzamide amides, carbamate, and doublet bands of the primary

amine of CHZ), 2981 (asym.  $sp^3$  str. vibration of  $CH_3$  and  $CH_2$  groups), 1700-1630 (broadband due to the overlap of C=O str. vibration of anilide, CHZ, anilide, and benzamide amides and carbamate), 1600, 1523 (aromatic C=C str.).

**4-(2-amino-3-phenylpropanamido)-N-(4-(2-hydrazinecarbonyl)hydrazine-1-carbonyl)benzyl) benzamide 3d**

Pale gray powder, yield 90%, m.p. 215-217,  $R_f$  0.81 (chloroform: methanol; 4: 6). FT-IR (ATR;  $\nu$ ,  $cm^{-1}$ ): 3363, 3300-3200 (broadband due to overlapping of str. vibration N-H bands of anilide and benzamide amides, and the doublet band of primary amine), 3086 (aromatic  $sp^2$  C-H str. vibration), 2989, 2912 (asym.  $sp^3$  str. vibration of  $CH_3$  &  $CH_2$  groups), 1685 (C=O str. vibration band of anilide amide), 1654 (C=O str. vibration of CHZ and benzamide amides), 1531 (aromatic C=C str. bands).  $C_{25}H_{27}N_7O_4$ ,  $^1H$ NMR ( $\delta$ , ppm): 10.33 (s, NH, 1H), 9.08 (s,  $NH_2$ , 2H), 8.96 (s, NH, H), 7.7 (s, NH, 1H), 7.2 (s, NH, 1H), 7.14 (s, NH, 1H), 7.8-7.2 (m, aromatic  $CH_2$  and CH, 13H), 4.5 (s,  $NH_2$ , 2H), 4.45 (t, CH, 1H), 2.83 (t, CH, 1H), 2.4 (d,

$CH_2$ , 2H).  $^{13}C$ NMR: 174.5 (C=ONH), 166.6 (C=ONH), 166.3 (C=ONH), 166.1 (CHZ C=O), 139.03-118.9 (aromatic), 57.6 (CH- $NH_2$ ), 42.8 ( $CH_2$ -NH), 41.4 ( $CH_2$ ).

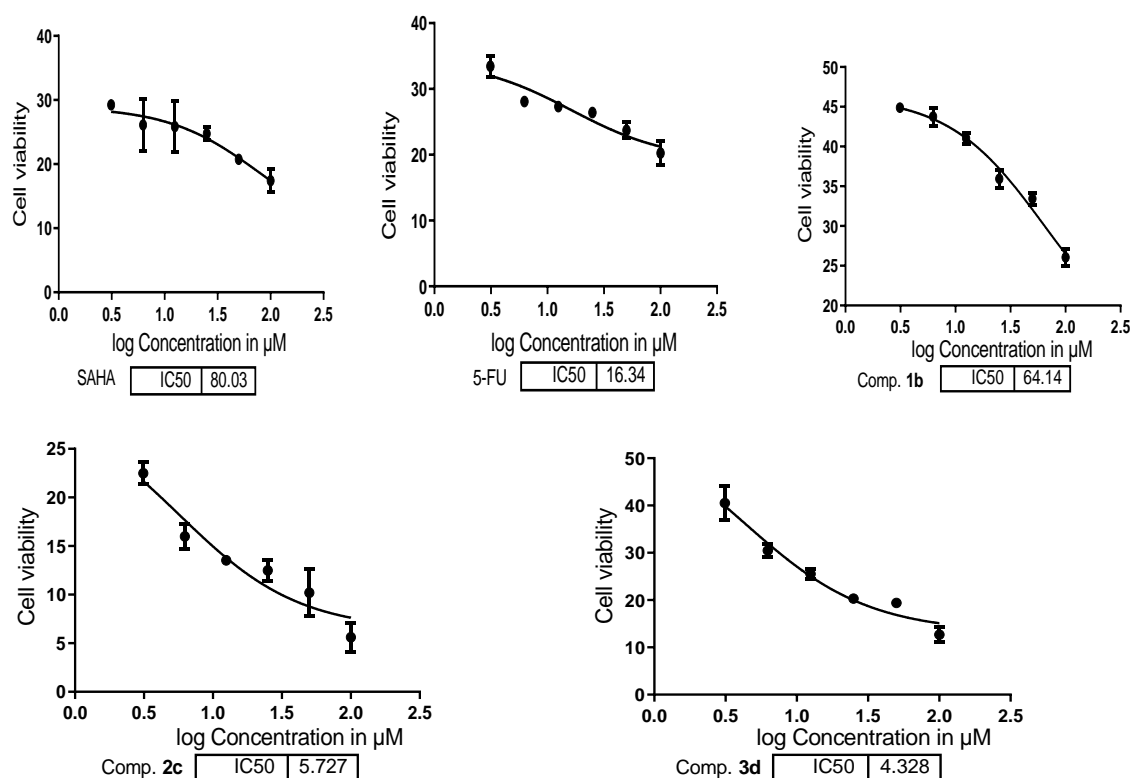
**3.3. Cytotoxicity study**

Compounds **1b**, **2c**, and **3d** were tested *in vitro* for their antiproliferative activity against breast cancer cell line (MCF7) and against normal human fibroblast-derived adipose tissue (NHF) to compare their cytotoxic effect with two reference standard chemotherapeutic agents (5-FU and SAHA). The rationale for choosing these two agents is due to the clinical use of 5-FU and SAHA in the treatment of breast cancer. Additionally, SAHA is the first HDAC inhibitor acquired FDA approval [37, 38]. All the compounds were tested at micromolar concentrations (3.125, 6.25, 12.5, 25, 50, 100  $\mu$ M).  $IC_{50}$  values of the tested compounds against MCF7 and NHF were analyzed by GraphPad Prism 9 software and listed in table 2. The statistically analyzed and visualized results of the MTT assay for MCF7 and NHF are shown in figures (6 to 8) and (9 to 11 respectively).

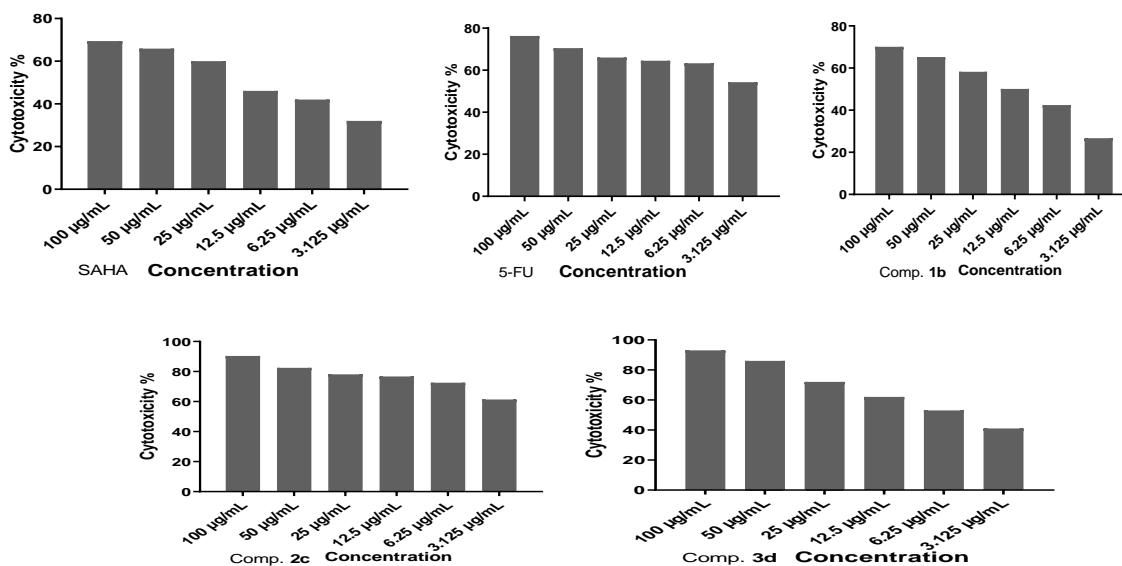
**Table 2.**  $IC_{50}$  values for the tested compounds. The values are represented by the mean  $\pm$ SD of triplicate measurements.

Comp.	$IC_{50}(\mu M) \pm SD$	P value	Significantly different (P value < 0.05)?
MCF7			
SAHA	80.03 $\pm$ 7.66	Reference	
5-FU	16.34 $\pm$ 0.323	Reference	
<b>1b</b>	64.14 $\pm$ 5.109	0.0563*	no
		0.0001**	yes, <
<b>2c</b>	5.727 $\pm$ 0.257	0.0001*	yes, >
		0.0003**	yes, >
<b>3d</b>	4.328 $\pm$ 0.223	0.0006*	yes, >
		0.003**	yes, >
NHF			
SAHA	26.74 $\pm$ 3.141	Reference	
5-FU	16.05 $\pm$ 0.323	Reference	
<b>1b</b>	25.75 $\pm$ 2.193	0.723*	no
		0.0097**	yes, <
<b>2c</b>	270.7 $\pm$ 13.26	0.0001*	yes, <
		0.0001**	yes, <
<b>3d</b>	75.3 $\pm$ 5.107	0.0003*	yes, <
		0.0001**	yes, <

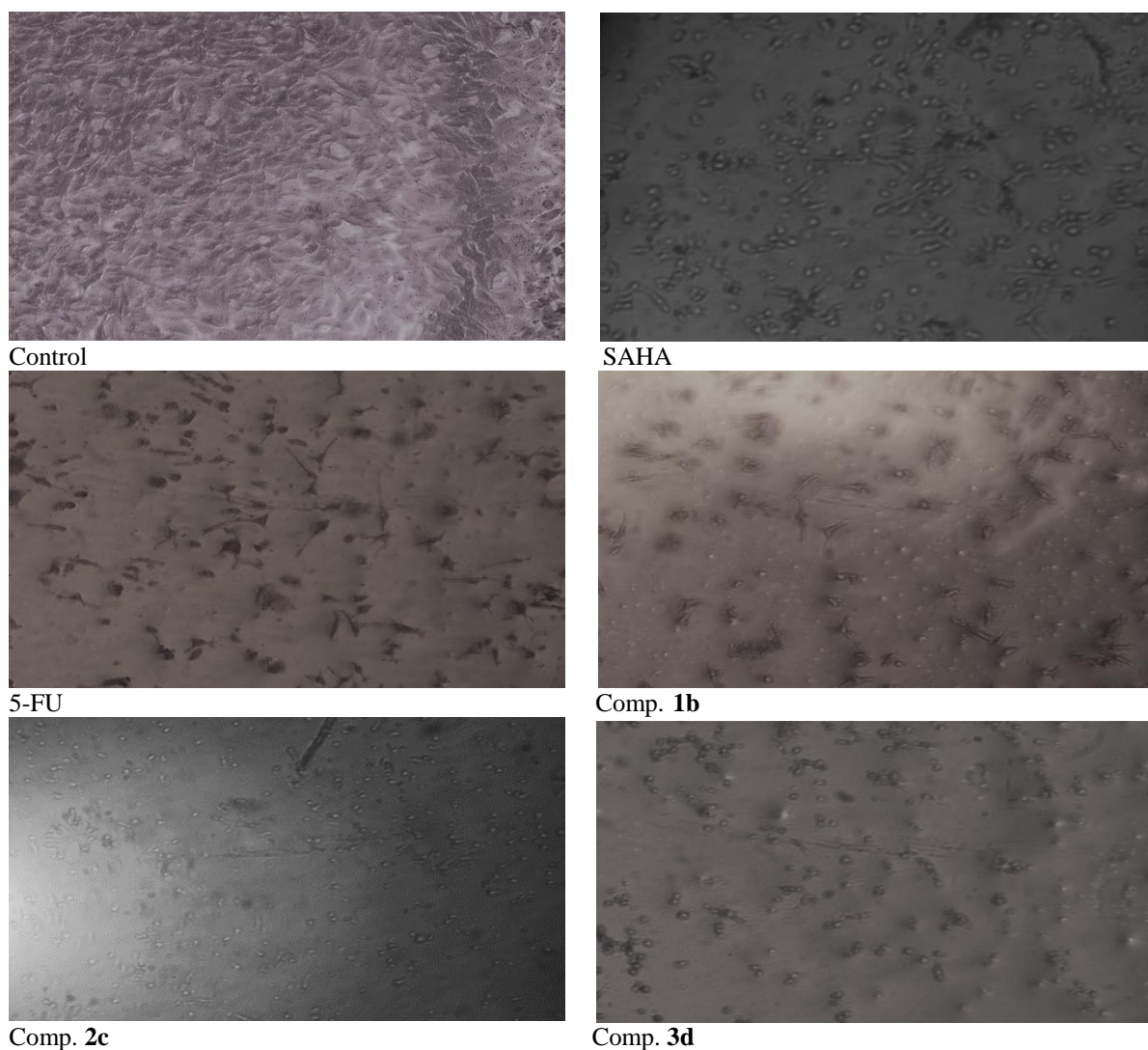
\* and \*\* represent that the compound is compared statistically with SAHA and 5-FU respectively. < and > represent that the compound has less and more growth inhibitory activity in comparison with the reference standard respectively



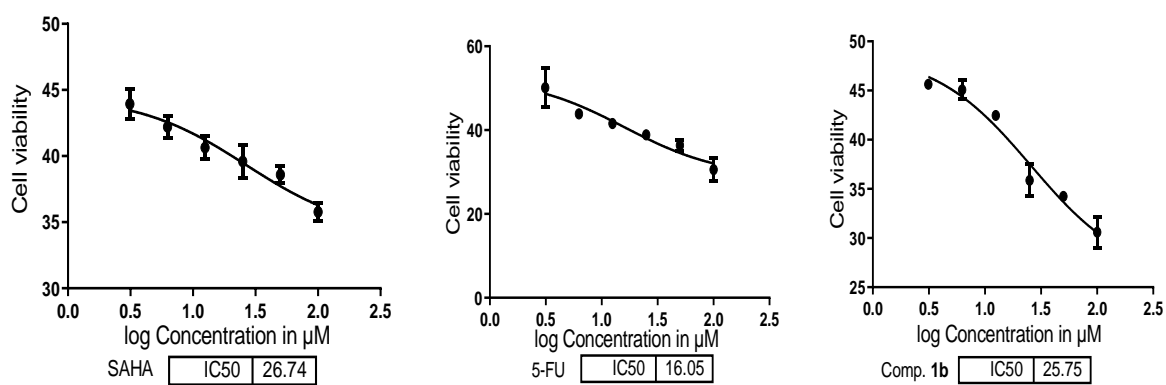
**Figure 6.**  $\text{IC}_{50}$  Values of the tested compounds against MCF7 as graphed by GraphPad Prism 9 software program.



**Figure 7.** Cytogram showing the cytotoxicity percentage of the tested compounds against MCF7 versus concentrations. Values are represented by the mean  $\pm$  SD of triplicate measurements.



**Figure 8.** Morphological pictures for MCF-7 cell line *in vitro* control cells and cytotoxicity under an inverted microscope, (10x).



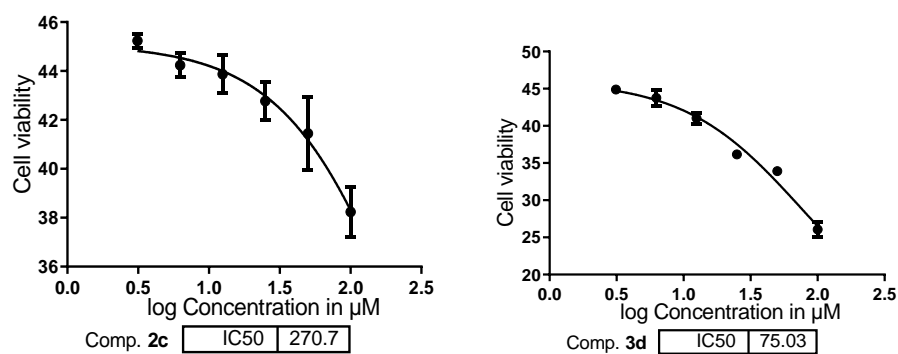


**Figure 9.** IC<sub>50</sub> Values of the tested compounds against NHF as graphed by GraphPad Prism 9 software program.

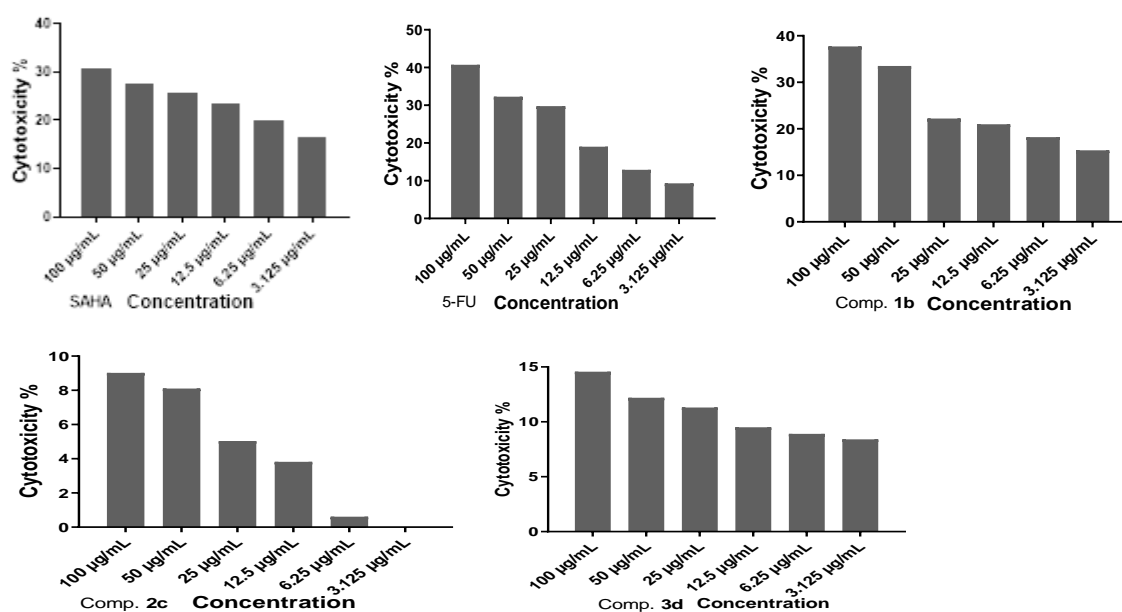
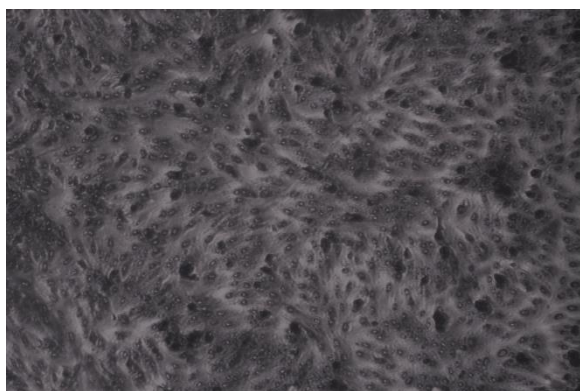
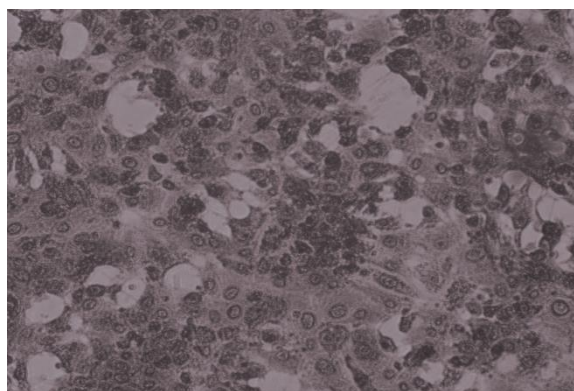


**Figure 10.** Cytogram showing the cytotoxicity percentage of the tested compounds against NHF versus concentrations. Values are represented by the mean  $\pm$  SD of triplicate measurements.



Control



SAHA

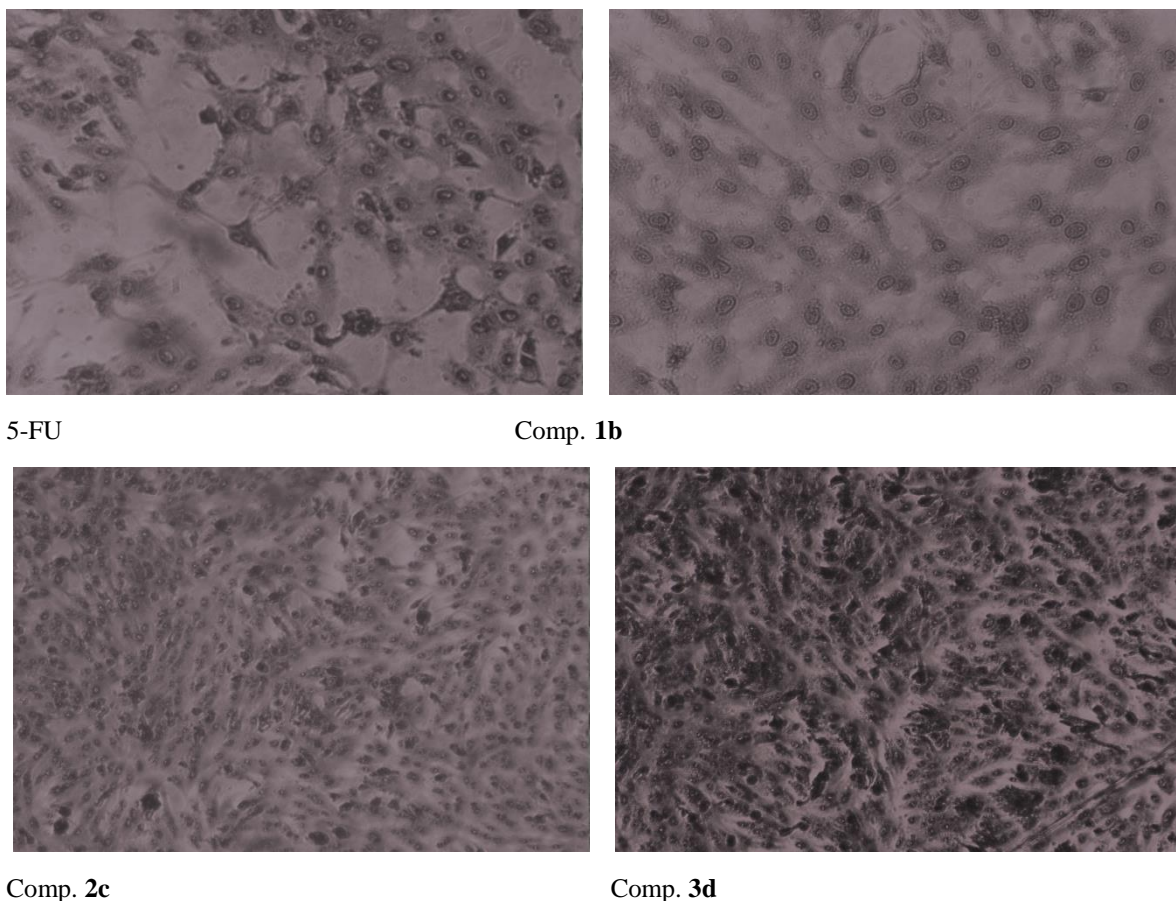


**Figure 11.** Morphological pictures for NHF cell line *in vitro* control cells and cytotoxicity under an inverted microscope, (10x).

Regarding MCF7, compound **3d** showed the highest cytotoxic effect among the tested compounds. Interestingly, two of the synthesized compounds (**2c** and **3d**) showed significantly higher cytotoxic activity than the reference standard agents ( $IC_{50}$ = 5.727 and 4.328  $\mu$ M for **2c** and **3d** in comparison to 80.03 and 16.34  $\mu$ M for SAHA and 5-FU). Compound **1b** showed no significant difference in comparison with SAHA ( $IC_{50}$ = 64.14,  $p>0.05$ ) and significantly lower cytotoxic activity than 5-FU (table 2). It's worth mentioning that at the lowest concentration (3.125  $\mu$ M), compound **2c** showed the highest percentage (>60%) of cytotoxicity (higher than SAHA and 5-FU) among the tested compounds as shown in figure 7.

Regarding NHF, compound **2c** showed the lowest cytotoxic effect among the tested compounds. Additionally, **2c** and **3d** showed significantly lower cytotoxic activity than the other tested compounds including SAHA and 5-FU ( $IC_{50}$ = 270.7 and 75.3  $\mu$ M for **2c** and **3d** in comparison to 26.74 and 16.05  $\mu$ M for SAHA and 5-FU respectively). Interestingly, compound **2c** showed a very low percentage of cytotoxicity (near zero) at the lowest concentration

(3.125  $\mu$ M) as shown in figure 10. The low toxicity of compound **2c** at low concentrations could be due to the higher receptor-mediated uptake of this compound by cancer cells rather than normal cells., This is can be explained by the important role of biotin as an exogenous micronutrient that is highly needed by cancer cells [39] with consequent high uptake by these cells which leads to improving the internalization of compound **2c** and achieving higher intracellular concentration and conferring targetability[40].

Cell line results were consistent with the docking study results. For example, compounds **2c** and **3d** displayed the highest PLP scores on HDAC 10 (93.89 and 114.52 respectively) and compound **1b** displayed the lowest scores for HDAC 2 and 10 among the three docked compounds. However, the role of biomolecules couldn't be predicted by the docking study. The high antiproliferative activity against MCF7 and low cytotoxic effect against NHF cell lines of compounds **3d** and **2c** could be due to the higher biomolecule-mediated uptake (by receptor-mediated internalization) of these compounds by MCF7 cells than NHF (which may improve their targetability).

This assumption couldn't be applied to compound **1b** because it lacks a conjugated biomolecule. From a structural point of view, compounds **2c** and **3d** generally are biomolecule-linked compound **1b**. Therefore, it is obvious that the high improvement in inhibitory activity against MCF7 and low toxicity against NHF cell lines is due to linking compound **1b** with a biomolecule (biotin and Phe).

#### 4. Conclusion

The target compounds (**1b**, **2c**, and **3d**) were synthesized successfully starting from benzoic acid, biotin, and Phe respectively. Compounds **2c** and **3d** showed a higher cytotoxic effect than SAHA and 5-FU against MCF7 and lower than them against NHF. Therefore, improving the antiproliferative activity against cancer cells and reducing the toxic effect against the normal cells of the new HDACIs (conferring targetability to cancer cells) could be objectively achieved by linking them to a biomolecule. Additionally, compound **1b** showed comparable results to SAHA, this finding indicates that CHZ could successfully replace the hydroxamate moiety and is considered a good candidate for designing new HDACIs. These findings will encourage us to extend our future researches to include studying the effect of the linked biomolecules on the pharmacokinetic profile of HDACIs such as oral bioavailability and water solubility which is important in the preparation of injectable dosage forms and extend the *in vitro* MTT study to include other cell lines and performing an *in vivo* toxicity study. Additionally, studying the *in vivo* pharmacokinetic effect of CHZ moiety (such as metabolism) to confer its safety and bypass the pharmacokinetic limitations of hydroxamate moiety.

#### Conflicts of interest

The authors declare no conflict of interest.

#### Acknowledgement

The authors would like to express their special thanks and gratitude to the staff of the spectral analysis lab, department of pharmaceutical chemistry, College of Pharmacy, University of Baghdad, for their valuable help and patience.

#### References

- [1] Y. Tian, Z. Xie, and C. Liao, "Design, synthesis and anticancer activities of novel dual poly(ADP-ribose) polymerase-1/histone deacetylase-1 inhibitors," *Bioorganic and Medicinal Chemistry Letters*, vol. 30, no. 8, p. 127036, Apr. 2020, doi: 10.1016/j.bmcl.2020.127036.
- [2] S. Kandasamy *et al.*, "Design and synthesis of imidazole based zinc binding groups as novel small molecule inhibitors targeting Histone deacetylase enzymes in lung cancer," *Journal of Molecular Structure*, vol. 1214, p. 128177, Aug. 2020, doi: 10.1016/j.molstruc.2020.128177.
- [3] T. Eckschlager, J. Plch, M. Stiborova, and J. Hrabeta, "Histone Deacetylase Inhibitors as Anticancer Drugs," *International Journal of Molecular Sciences 2017, Vol. 18, Page 1414*, vol. 18, no. 7, p. 1414, Jul. 2017, doi: 10.3390/IJMS18071414.
- [4] H. CC *et al.*, "Suberoylanilide hydroxamic acid represses glioma stem-like cells," *Journal of biomedical science*, vol. 23, no. 1, pp. 1–12, Nov. 2016, doi: 10.1186/S12929-016-0296-6.
- [5] G. Li, Y. Tian, and W.-G. Zhu, "The Roles of Histone Deacetylases and Their Inhibitors in Cancer Therapy," *Frontiers in Cell and Developmental Biology*, vol. 0, p. 1004, Sep. 2020, doi: 10.3389/FCELL.2020.576946.
- [6] L. Cappellacci, D. R. Perinelli, F. Maggi, M. Grifantini, and R. Petrelli, "Recent Progress in Histone Deacetylase Inhibitors as Anticancer Agents," *Current Medicinal Chemistry*, vol. 27, no. 15, pp. 2449–2493, Oct. 2018, doi: 10.2174/0929867325666181016163110.
- [7] A. K. Meka *et al.*, "Enhanced Solubility, Permeability and Anticancer Activity of Vorinostat Using Tailored Mesoporous Silica Nanoparticles," *Pharmaceutics*, vol. 10, no. 4, Dec. 2018, doi: 10.3390/PHARMACEUTICS10040283.
- [8] M. M. Abdel-Atty, N. A. Farag, R. A. T Serya, K. A. M Abouzid, S. Mowafy, and K. A. M, "Molecular design, synthesis and *in vitro* biological evaluation of thienopyrimidine-hydroxamic acids as chimeric kinase HDAC inhibitors: a challenging approach to combat cancer," 2021, doi: 10.1080/14756366.2021.1933465.
- [9] M. Manal, M. J. N. Chandrasekar, J. Gomathi Priya, and M. J. Nanjan, "Inhibitors of histone deacetylase as antitumor agents: A critical review," *Bioorganic Chemistry*, vol. 67, pp. 18–42, Aug. 2016, doi: 10.1016/J.BIOORG.2016.05.005.
- [10] C.-F. YY *et al.*, "Design and synthesis of potent dual inhibitors of JAK2 and HDAC based on fusing the pharmacophores of XL019 and vorinostat," *European journal of medicinal chemistry*, vol. 158, pp. 593–619, Oct. 2018, doi: 10.1016/J.EJMECH.2018.09.024.

- [11] L. Ning, X. Rui, W. Bo, and G. Qing, "The critical roles of histone deacetylase 3 in the pathogenesis of solid organ injury," *Cell Death & Disease* 2021 12:8, vol. 12, no. 8, pp. 1–13, Jul. 2021, doi: 10.1038/s41419-021-04019-6.
- [12] M. Montalvo-Casimiro, R. González-Barrios, M. A. Meraz-Rodriguez, V. T. Juárez-González, C. Arriaga-Canon, and L. A. Herrera, "Epidrug Repurposing: Discovering New Faces of Old Acquaintances in Cancer Therapy," *Frontiers in Oncology*, vol. 0, p. 2461, Nov. 2020, doi: 10.3389/FONC.2020.605386.
- [13] B. Pitt, N. R. Sutton, Z. Wang, S. N. Goonewardena, and M. Holinstat, "Potential repurposing of the HDAC inhibitor valproic acid for patients with COVID-19," *European Journal of Pharmacology*, vol. 898, p. 173988, May 2021, doi: 10.1016/J.EJPHAR.2021.173988.
- [14] A. Citarella and N. Micale, "Peptidyl Fluoromethyl Ketones and Their Applications in Medicinal Chemistry," *Molecules* 2020, Vol. 25, Page 4031, vol. 25, no. 17, p. 4031, Sep. 2020, doi: 10.3390/MOLECULES25174031.
- [15] R. Sarkar, S. Banerjee, S. A. Amin, N. Adhikari, and T. Jha, "Histone deacetylase 3 (HDAC3) inhibitors as anticancer agents: A review," *European Journal of Medicinal Chemistry*, vol. 192, p. 112171, Apr. 2020, doi: 10.1016/J.EJMECH.2020.112171.
- [16] Y. C et al., "Structure optimization and preliminary bioactivity evaluation of N-hydroxybenzamide-based HDAC inhibitors with Y-shaped cap," *Bioorganic & medicinal chemistry*, vol. 26, no. 8, pp. 1859–1868, May 2018, doi: 10.1016/J.BMC.2018.02.033.
- [17] F. Yang, N. Zhao, D. Ge, and Y. Chen, "Next-generation of selective histone deacetylase inhibitors," 2019, doi: 10.1039/c9ra02985k.
- [18] L. Ruess and D. C. Müller-Navarra, "Essential Biomolecules in Food Webs," *Frontiers in Ecology and Evolution*, vol. 0, p. 269, Jul. 2019, doi: 10.3389/FEVO.2019.00269.
- [19] N. Boodhun, "Seeing is believing: structures and functions of biological molecules," <https://doi.org/10.2144/btn-2017-0123>, vol. 64, no. 4, pp. 143–146, Apr. 2018, doi: 10.2144/BTN-2017-0123.
- [20] R. P. Bhole, S. Jadhav, Y. B. Zambare, R. v. Chikhale, and C. G. Bonde, "Vitamin-anticancer drug conjugates: a new era for cancer therapy.," *Journal of the Faculty of Pharmacy of Istanbul University*, vol. 50, no. 3, pp. 312–323, Dec. 2020, Accessed: Aug. 09, 2021. [Online]. Available: <https://go.gale.com/ps/i.do?p=HRCA&sw=w&issn=03677524&v=2.1&it=r&id=GALE%7CA649245102&sid=googleScholar&linkacces=fulltext>
- [21] M. F. Seifu and L. K. Nath, "Polymer-Drug Conjugates: Novel Carriers for Cancer Chemotherapy," <https://doi.org/10.1080/03602559.2018.1466172>, vol. 58, no. 2, pp. 158–171, Jan. 2018, doi: 10.1080/03602559.2018.1466172.
- [22] Z.-M. Li, T.-L. Zhang, L. Yang, Z.-N. Zhou, and J.-G. Zhang, "Synthesis, crystal structure, thermal decomposition, and non-isothermal reaction kinetic analysis of an energetic complex: [Mg(CHZ)3](ClO4)2 (CHZ = carbonylhydrazide)," <https://doi.org/10.1080/00958972.2011.643790>, vol. 65, no. 1, pp. 143–155, Jan. 2011, doi: 10.1080/00958972.2011.643790.
- [23] V. BS, H. KM, L. K, and R. J, "Amino acids as promoiety in prodrug design and development," *Advanced drug delivery reviews*, vol. 65, no. 10, pp. 1370–1385, Oct. 2013, doi: 10.1016/J.ADDR.2012.10.001.
- [24] "RCSB PDB: Homepage." <https://www.rcsb.org/> (accessed Oct. 07, 2021).
- [25] M. R. Al-Nakeeb and T. N.-A. Omar, "Synthesis, Characterization and Preliminary Study of the Anti-Inflammatory Activity of New Pyrazoline Containing Ibuprofen Derivatives," *Iraqi Journal of Pharmaceutical Sciences*, vol. 28, no. 1, 2019, Accessed: Aug. 26, 2021. [Online]. Available: <https://www.iasj.net/iasj/article/164985>
- [26] S. M. Alwan and A. H. Kadhim, "Synthesis of New Cephalosporins of Expected Improved Activity and Resistance Against Lactamases," *Iraqi Journal of Pharmaceutical Sciences* ( P-ISSN: 1683 - 3597 , E-ISSN: 2521 - 3512), vol. 23, no. 2, pp. 24–32, 2014, doi: 10.31351/VOL23ISS2PP24-32.
- [27] A. T. Sulaiman and S. W. Sarsam, "Synthesis, Characterization and Antibacterial Activity Evaluation of New Indole-Based Derivatives," *Iraqi Journal of Pharmaceutical Sciences* ( P-ISSN: 1683 - 3597 , E-ISSN: 2521 - 3512), vol. 29, no. 1, pp. 207–215, Jun. 2020, doi: 10.31351/VOL29ISS1PP207-2015.
- [28] "Design, Synthesis and Preliminary Antimicrobial Evaluation of New Derivatives of Cephalexin - Google Search." <https://www.google.com/search?q=Design%2>

- C+Synthesis+and+Preliminary+Antimicrobia  
l+Evaluation+of+New+Derivatives+of+Ceph  
alexin&oq=Design%2C+Synthesis+and+Prel  
iminary+Antimicrobial+Evaluation+of+New  
+Derivatives+of+Cephalexin&aqs=chrome..6  
9i57j69i60.748j0j4&sourceid=chrome&ie=U  
TF-8 (accessed Oct. 11, 2021).
- [29] A. M. Al-Shammari *et al.*, "Establishment and characterization of a receptor-negative, hormone-nonresponsive breast cancer cell line from an Iraqi patient," *Breast Cancer: Targets and Therapy*, vol. 7, p. 223, Aug. 2015, doi: 10.2147/BCTT.S74509.
- [30] B. SR and G. A, "The Characters of Graphene Oxide Nanoparticles and Doxorubicin Against HCT-116 Colorectal Cancer Cells In Vitro," *Journal of gastrointestinal cancer*, 2021, doi: 10.1007/S12029-021-00625-X.
- [31] S. A. Abdullah, A. M. Al-Shammari, and S. A. Lateef, "Attenuated measles vaccine strain have potent oncolytic activity against Iraqi patient derived breast cancer cell line," *Saudi Journal of Biological Sciences*, vol. 27, no. 3, pp. 865–872, Mar. 2020, doi: 10.1016/J.SJBS.2019.12.015.
- [32] A.-S. AM, J. RDA, and H. MF, "Combined therapy of oncolytic Newcastle disease virus and rhizomes extract of Rheum ribes enhances cancer virotherapy in vitro and in vivo," *Molecular biology reports*, vol. 47, no. 3, pp. 1691–1702, Mar. 2020, doi: 10.1007/S11033-020-05259-Z.
- [33] M. S. Jabir *et al.*, "Green synthesis of silver nanoparticles from Eriobotrya japonica extract: a promising approach against cancer cells proliferation, inflammation, allergic disorders and phagocytosis induction," <https://doi.org/10.1080/21691401.2020.1867152>, vol. 49, no. 1, pp. 48–60, 2021, doi: 10.1080/21691401.2020.1867152.
- [34] W. A *et al.*, "Histone Deacetylase Inhibitors and Phenotypical Transformation of Cancer Cells," *Cancers*, vol. 11, no. 2, Jan. 2019, doi: 10.3390/CANCERS11020148.
- [35] "Case: What is the difference between the GoldScore, ChemScore, ASP and ChemPLP scoring functions provided with GOLD? - The Cambridge Crystallographic Data Centre (CCDC)." <https://www.ccdc.cam.ac.uk/support-and-resources/support/case/?caseid=5d1a2fc0-c93a-49c3-a8e2-f95c472dcff0> (accessed Sep. 26, 2021).
- [36] E. D. Boittier, Y. Y. Tang, M. E. Buckley, Z. P. Schuurs, D. J. Richard, and N. S. Gandhi, "Assessing Molecular Docking Tools to Guide Targeted Drug Discovery of CD38 Inhibitors," *International Journal of Molecular Sciences 2020, Vol. 21, Page 5183*, vol. 21, no. 15, p. 5183, Jul. 2020, doi: 10.3390/IJMS21155183.
- [37] R. Ponce-Cusi and G. M. Calaf, "Apoptotic activity of 5-fluorouracil in breast cancer cells transformed by low doses of ionizing  $\alpha$ -particle radiation," *International Journal of Oncology*, vol. 48, no. 2, pp. 774–782, Feb. 2016, doi: 10.3892/IJO.2015.3298.
- [38] A. Wawruszak, L. Borkiewicz, E. Okon, W. Kukula-Koch, S. Afshan, and M. Halasa, "Vorinostat (SAHA) and Breast Cancer: An Overview," *Cancers 2021, Vol. 13, Page 4700*, vol. 13, no. 18, p. 4700, Sep. 2021, doi: 10.3390/CANCERS13184700.
- [39] S. Collina, "New Perspectives in Cancer Therapy: The Biotin-Antitumor Molecule Conjugates," *Medicinal Chemistry*, vol. 5, no. 1, 2014, doi: 10.4172/2161-0444.S1-004.
- [40] X. Song, P. L. Lorenzi, C. P. Landowski, B. S. Vig, J. M. Hilfinger, and G. L. Amidon, "Amino acid ester prodrugs of the anticancer agent gemcitabine: synthesis, bioconversion, metabolic bioevasion, and hPEPT1-mediated transport," *Molecular pharmaceuticals*, vol. 2, no. 2, pp. 157–167, Mar. 2005, doi: 10.1021/MP049888E.